HHS Public Access

Author manuscript

Hepatology. Author manuscript; available in PMC 2019 October 01.

Published in final edited form as:

Hepatology. 2018 October ; 68(4): 1519–1533. doi:10.1002/hep.29915.

Disruption of renal arginine metabolism promotes kidney injury in hepatorenal syndrome

Zoltan V. Varga[1,*], **Katalin Erdelyi**[1,*], **Janos Paloczi**[1,*], **Resat Cinar**[2], **Zsuzsanna K. Zsengeller**[3], **Tony Jourdan**[2], **Csaba Matyas**[1], **Balazs Tamas Nemeth**[1], **Adrien Guillot**[4], **Xiaogang Xiang**[4], **Adam Mehal**[1], **George Hasko**[5], **Isaac E. Stillman**[6], **Seymour Rosen**[6], **Bin Gao**[4], **George Kunos**[2], and **Pal Pacher**[1]

[1]Laboratory of Cardiovascular Physiology and Tissue Injury, National Institutes of Health/NIAAA, Bethesda, MD 20852, USA

[2]Laboratory of Physiological Studies, National Institutes of Health/NIAAA, Bethesda, MD 20852, USA

[3]Department of Medicine, Division of Nephrology, Beth Israel Deaconess Medical Center, Boston, MA 02215, USA

[4]Laboratory of Liver Diseases, National Institutes of Health/NIAAA, Bethesda, MD 20852, USA

[5]Department of Anesthesiology, Columbia University, New York, NY, 10032, USA

[6]Department of Pathology, Beth Israel Deaconess Medical Center, Boston, MA 02215, USA

Abstract

Tubular dysfunction is an important feature of renal injury in hepatorenal syndrome (HRS) in patients with end-stage liver disease. The pathogenesis of kidney injury in HRS is elusive, and there are no clinically relevant rodent models of HRS. We investigated the renal consequences of bile-duct ligation (BDL)-induced hepatic and renal injury in mice *in vivo* by using biochemical assays, real-time PCR, Western blot, mass spectrometry, histology and electron microscopy.

BDL resulted in time-dependent hepatic injury and hyperammonemia which were paralleled by tubular dilation and tubulointerstitial nephritis with marked upregulation of lipocalin-2, KIM-1 and osteopontin. Renal injury was associated with dramatically impaired microvascular flow and decreased endothelial nitric oxide synthase (eNOS) activity. Gene expression analyses signified proximal tubular epithelial injury, tissue hypoxia, inflammation, and activation of the fibrotic gene program. Marked changes in renal arginine metabolism (upregulation of arginase-2 and downregulation of argininosuccinate synthase 1), resulted in decreased circulating arginine levels. Arginase-2 knockout mice were partially protected from BDL-induced renal injury and had less

Contact: Pal Pacher, MD, PhD, FAHA, FACC, Laboratory of Cardiovascular Physiology and Tissue Injury, 5625 Fishers Lane, Room 2N-17; Bethesda, MD 20892-9413, Phone: (301)-443-4830; pacher@mail.nih.gov.

*These authors contributed equally to this work.

Author Contributions: Z.V.V., E.K. and P.P. conceived and designed research; Z.V.V., K.E., J.P., R.C., C.M., B.T.N., T.J., A.G., A.M., X.X., Z.K.Z. performed experiments; Z.V.V., K.E., J.P. analyzed data; Z.V.V., R.C., B.G., G.K., I.E.S., S.R., and P.P. interpreted results of experiments; Z.V.V. prepared figures; Z.V.V and P.P. drafted manuscript; Z.V.V., T.J., G.H., B.G., G.K., and P.P. edited and revised manuscript. All authors approved final version of the manuscript.

Conflict of interest disclosure: All authors declare no conflict of interest.

impairment in microvascular function. In human cultured proximal tubular epithelial cells hyperammonemia *per se* induced upregulation of arginase-2 and markers of tubular cell injury.

Conclusions—We propose that hyperammonemia may contribute to impaired renal arginine metabolism, leading to decreased eNOS activity, impaired microcirculation, tubular cell death, tubulointerstitial nephritis and fibrosis. Genetic deletion of arginase-2 partially restores microcirculation and thereby alleviates tubular injury. We also demonstrate that BDL in mice is an excellent, clinically relevant model to study the renal consequences of HRS.

Keywords

liver failure; cirrhosis; cholemic nephropathy; portal hypertension; kidney failure

Introduction

Chronic liver diseases and their complications including liver cirrhosis are major public health concerns worldwide, due to the associated significant morbidity and mortality[1]. Acute kidney injury (AKI) in hepatorenal syndrome (HRS) is a potentially lethal complication of liver failure and is characterized by a rapid decline in renal function in cirrhotic patients. Although, the definition and diagnostic criteria of type-1 and type-2 HRS and AKI-HRS are in constant flux[2], it is now generally accepted that a diagnosis of HRS can be made when renal dysfunction develops in patients with advanced cirrhosis and ascites[3]. HRS is present in 20–50% of hospitalized cirrhotic patients[4] and is considered a serious complication often precipitated by bleeding, bacterial/viral infections or dehydration. AKI in HRS has a poor prognosis and is an important predictor of short-term mortality in patients with cirrhosis[5] and their survival and outcome when they undergo liver transplantation[6].

Our understanding of the pathogenesis of kidney dysfunction in advanced liver failure is limited. There are no perfect animal models for HRS, which likely reflects the difficulty in inducing advanced liver failure in experimental animals without the use of poisonous hepatotoxins (e.g. carbon tetrachloride, acetaminophen, D-galactosamine, thioacetamide, etc.) which may damage the kidneys directly. Nonetheless, clinical observations point to the critical pathogenic role of severe vasodilation in the splanchnic vasculature seen in decompensated liver failure, which, in turn, induces compensatory vasoconstriction, leading to renal circulatory derangement[7]. Other theories focus on the role of aggravated systemic inflammation and bacterial translocation seen in decompensated cirrhosis[8], and on the importance of cardiac[9] and adrenal insufficiency[10]. A separate entity described in patients suffering from biliary obstruction is cholemic nephropathy, which results from the toxic effects of bile acids and bilirubin casts on the tubular apparatus[11–13]. All of the aforementioned extrarenal factors likely contribute to the development of kidney injury, while intrarenal mechanisms that may lead to tubular cell death in HRS have not yet been identified.

Our lack of understanding of its pathogenesis aside, AKI-HRS is probably one of the most challenging complication of liver cirrhosis to treat. Its preferred treatment is liver transplantation, but many patients unfortunately die before transplantation due to organ

shortage and the short survival associated with AKI-HRS. Supportive treatment is aimed to improve renal function before transplantation, as patients with AKI-HRS receiving liver transplantation have greater mortality than those with other diagnoses[14]. Current therapeutic options are limited and usually target extrarenal triggers of HRS, for example by trying to correct the hypovolemia and splanchnic vasodilation through the use of volume expanders and somatostatin and vasopressin analogues.

Therefore, we aimed to develop and characterize a pathologically relevant mouse model of AKI-HRS without the use of hepatotoxins, and to study intrarenal mechanisms that might contribute to the development of tubular injury. We report that bile duct-ligated mice develop tubular injury, tubulointerstitial nephritis and fibrosis that closely resemble the histological features seen in patients suffering from AKI-HRS. In this model, disruption of renal arginine metabolism contributes to the impairment of the renal microcirculation and tubular injury. Genetic deletion of ARG2 partially protects against BDL-induced HRS, which implicates a novel intrarenal disease-specific pharmacological target for alleviating kidney injury and delaying its progression to HRS.

Materials and Methods

Animals

All animal protocols conformed to the National Institutes of Health (NIH) guidelines and were approved by the Institutional Animal Care and Use Committee of the National Institute on Alcohol Abuse and Alcoholism (Bethesda, MD). Ten to 15 week-old male C57BL/6J or *Arg2*$^{-/-}$ mice were obtained from the Jackson Laboratory (Bar Harbor, ME, USA). Wild-type (WT) and *Arg2*$^{-/-}$ mice were used in the study.

Bile Duct-Ligation Model

BDL surgery was performed as described in detail in the Supplementary Methods[15].

Indicators of Kidney and Liver Injury

Serum levels of alanine aminotransferase (ALT), alkaline phosphatase (ALKP), blood urea nitrogen (BUN), urinary urea nitrogen, creatinine, and ammonia were measured using a clinical chemistry analyzer - Idexx VetTest 8008 (Idexx Laboratories, Westbrook, ME, USA). Urinary creatinine, urinary sodium were measured with colorimetric kits from Biovision Inc. (Milpitas, CA., USA).

Serum levels of the tubular injury markers, kidney injury molecule-1 (KIM1), and osteopontin were measured by commercially available ELISA kits (Cat#MKM100, MOST00, R&D Systems, Minneapolis, MN, USA).

Arterial and Microvascular Flow Measurements

Blood flow in the renal artery was measured using a flow probe (Transonic Systems Inc. Ithaca, NY, USA), renal microcirculation was assessed by the laser speckle contrast approach as described in the supplementary methods.

cGMP, arginase and eNOS activity measurements are described in the supplemental methods

Reverse Transcription and Real-Time PCR analyses were performed as previously described[15]. Primer sequences are provided in Supplementary Table 1.

Histology, Immunohistochemistry, Transmission Electron Microscopy were performed as described in the supplementary methods[15].

Determination of Serum Free Amino Acid Content

Free amino acids in serum were measured by tandem mass spectrometry (LC-MS/MS) as described in the Supplementary methods.

Western Blots

The details of Western blot detection of renal ARG1, ARG2, ASS1and HIF1-α proteins are provided in the supplementary methods.

Ammonia and Endotoxin Exposure of Cells

Culture and ammonia exposure of human renal proximal tubular epithelial cells (RPTEC) and human umbilical vein endothelial cells (HUVEC) are described in the supplementary methods.

Statistical Analysis

Values are represented as mean±S.E.M. Statistical analysis of the data was performed by one or two-way analysis of variance (ANOVA) followed by Tukey's post-hoc test for multiple comparisons, as appropriate. The analysis was conducted using GraphPad-Prism4 software. $P < 0.05$ was considered statistically significant.

Results

Bile duct-ligation leads to hepatic injury

We first characterized time-dependent changes of body weight and liver injury in the mouse BDL model (Fig. 1 and Suppl. Fig. 1). There was an apparent change in hepatic tissue architecture as early as 7 days post BDL characterized by pronounced biliary inflammation with scattered small necrotic foci and fibrosis predominantly localized around inflamed bile ducts. By day 14 post-ligation fibrosis spread to the liver parenchyma (Fig. 1A). The rapid onset of liver injury was paralleled by the increased expression of markers of fibrotic remodeling (*Tgfb1, Col1a1, Col3a1*) and inflammation (*Tnf, Ccl3, Cxcl2*) (Fig. 1B). Tissue injury was reflected by elevations of the serum alanine aminotransferase (ALT-marker of hepatocyte necrosis), and alkaline phosphatase (ALKP-marker of biliary injury) (Fig. 1C). Serum markers of renal dysfunction (blood urea nitrogen (BUN) and creatinine) were also increased (Fig. 1D) at 7 and/or 14 days after BDL, which prompted us to investigate the renal consequences of liver injury and to identify possible intrarenal causes for the kidney damage.

Bile duct-ligation leads to progressive tubular injury in the kidney

We observed progressive tubular damage in the cortical parts of the kidneys after BDL, associated with increased kidney/body weight ratio (Fig. 2A–C). Tubular injury was characterized by the markedly elevated circulating levels of kidney injury molecule 1 (KIM-1) and osteopontin, known biomarkers of acute kidney injury (Fig. 2D). Histological analyses provided further evidence for tubular injury in the form of dilated tubules containing protein casts at day 7 post-ligation (Fig. 2A). By day 14, massive tubular dilation with extensive cast formation became visible. The injured and dilated tubuli were strongly expressing lipocalin 2, a widely used biomarker for acute kidney injury. In addition, renal interstitial fibrosis that was not evident at day 7 became visible by day 14 (Fig. 2A). Transmission electron microscopy of tubular epithelial cells from sham operated mice showed normal mitochondrial morphology and distribution. In BDL mice sacrificed on postoperative day 7, proximal tubular cells had maintained brush border, and mitochondria of various size and shape were present (megamitochondria formation could be seen in some tubules, most likely because of altered microcirculation and progressively ischemic microenvironment). On postoperative day 14, when proximal tubules were greatly injured and dilated, the brush border was diminished/lost. Mitochondria were significantly decreased in number, due to an increase in autophagy. Those that remained were largely detectable within autophagolysosomes (Fig. 2B). Furthermore, the expression of markers of tubular injury (*Havcr1* - KIM-1, *Lcn2*- lipocalin-2, *Fabp1* – fatty acid binding protein 1, *Vim* - vimentin) was robustly increased (Fig. 2E left panel) in renal cortices from BDL mice. In contrast, there was a profound reduction in the expression of markers of proximal tubular cell function (*Lrp2* – megalin, and *Cubn* – cubilin – both involved in protein reabsorption; *Slc5a2* – known as SGLT2 - involved in glucose reabsorption; and *Slc34a1* – the proximal tubular specific sodium/phosphate cotransporter) (Fig. 2E right panel). We also found increased expression of several pro-inflammatory cytokines (*Il1b*, *Il6*, *Tnfa*, *Ccl2*, *Ccl3*, and *Cxcl2*) (Fig. 2F left panel) and pro-fibrotic genes (*Tgfb1*, *Col1a1*, and *Col3a1*)(Fig. 2F right panel).

Bile duct-ligation leads to microvascular injury in the kidney

Chronic interstitial and tubular cell hypoxia[16] as a result of microvascular dysfunction is a major trigger of tubular cell death, and is associated with the development of interstitial fibrosis[17, 18]. Therefore, we looked for changes in peritubular endothelial cells, and found that the fenestrations that were evident in the sham operated mice significantly diminished in BDL mice, in addition the endothelium became focally detached (Fig. 3A). We measured the blood flow in the renal artery using an ultrasonic probe as well as renal microvascular function, quantified by laser speckle contrast analysis in BDL and control mice. Blood flow through the renal artery was not significantly changed ($p= 0.35$) 14 days after BDL (0.33±0.02 mL/min) as compared to sham operated mice (0.37±0.04 mL/min). In contrast, there was a dramatic time-dependent reduction in microvascular flow in the kidneys of BDL mice, suggesting the involvement of hypoxia in the development of the kidney pathology seen (Fig. 3B,C). Parallel to the decreased microcirculation, we detected a significantly increased expression of *Hif1a,* the gene encoding the transcription factor hypoxia-inducible factor 1-α in the kidneys of BDL mice (Fig. 3D). In contrast, at the protein level we observed decreased phosphorylation of HIF1α (Fig. 3E) in the kidney of BDL mice that

likely results from chronic hypoxia. When dephosphorylated, HIF1α is unable to bind HIF1β, and thereby to enter the nucleus and induce the expression of hypoxia responsive genes(19, 20). Accordingly, gene expression of angiogenic factors, such as *Vegfa* (vascular endothelial growth factor A) and *Angpt1* (angiopoietin 1) decreased significantly by day 14 following BDL (Fig. 3D). In addition, the VEGF-A receptor *Kdr (*Kinase insert domain receptor) and the angiopoietin 1 receptor *Tie1* (Tyrosine kinase with immunoglobulin-like and EGF-like domains 1) were also expressed at significantly lower levels in the kidney of BDL compared to control mice (Fig. 3D). To further test if vascular inflammation contributes to microcirculatory dysfunction, we assessed the expression of vascular adhesion molecules. The renal expression of *Pecam1* and *Cdh5* (VE-cadherin) remained unchanged, whereas the expression of *Vcam1*, *Icam1*, *Sele*, and *Selp* was increased (Fig. 3F), suggesting increased renal vascular inflammation and consequent dysfunction.

Dissociation of renal arginine metabolism in bile duct-ligated mice

The kidney has a central role in systemic arginine metabolism, a process that is closely coupled to ammonia detoxification (also known as the urea cycle) (Fig. 4A). Renal arginine synthesis is a major endogenous source of arginine, and the urea cycle enzymes responsible for arginine synthesis, argininosuccinate synthase (ASS1) and lyase (ASL) are highly and almost exclusively expressed in kidney[21]. In healthy humans, the liver controls ammonia metabolism via the urea cycle, while the kidney is responsible for urinary ammonium ion excretion (by breaking down glutamine via the kidney specific glutaminase)[22]. Liver failure is often associated with disturbed ammonia homeostasis and the consequent development of hyperammonemia. Serum ammonia levels were markedly increased in BDL mice (Fig. 4B). It is known that the interorgan trafficking of ammonium is altered in hepatic disease[23], however, the extent to which renal urea cycle and arginine metabolism are modified by hyperammonemia is not known. We found decreased expression of glutamine synthase (*Glul*) and glutamate dehydrogenase (*Glud*) both in the liver and kidney of BDL mice, suggesting impaired ammonia detoxification by these two pathways (Fig. 4C). The liver showed decreased expression of the critical urea cycle enzyme ornithine transcarbamylase (*Otc*), while there was a slight induction of arginase-1 (*Arg1*), and a marked induction of arginase-2 (*Arg2*) expression (Fig. 4C upper panel). In contrast, the kidney did not express the urea cycle enzymes carbamoyl phosphate synthetase 1 (*Cps1*) and ornithine transcarbamylase (*Otc*). However, the expression of argininosuccinate synthase 1 (*Ass1*) and argininosuccinate lyase (*Asl*) was markedly reduced (Fig. 4C lower panel, and D), both being involved in *de novo* arginine synthesis. Surprisingly, the expression of both arginase isoforms markedly increased both at the mRNA (Fig. 4C lower panel) and protein levels (Fig. 4.E), suggesting decreased *de novo* synthesis and enhanced renal breakdown of arginine. The cell type-specific expression of the arginase isoforms was analyzed by immunohistochemistry (Fig. 4.F). Arginase-1 was localized around some damaged and dilated tubules 14 days after BDL (Fig. 4.F upper panels), while arginase-2 displayed a diffuse, tubular-specific staining that progressively increased after BDL (Fig. 4F lower panels).

To see if changes in the expression of these key urea cycle enzymes result in altered levels of serum free amino acids, we measured amino acids (see Supplementary Table 2.) and amino

acid intermediates of arginine metabolism by mass spectrometry, as illustrated in Fig. 5. We detected a marked drop in serum arginine levels (Fig. 5A) that paralleled significant increases in ornithine and citrulline levels, indicating increased breakdown of arginine both by arginases and nitric oxide synthases (NOS). Serum aspartate and glutamate levels were not altered, however, we found a slight but significant increase in serum glutamine levels, the latter likely being a result of increased skeletal muscle glutamine synthesis (Fig. 4A and Suppl. Fig. 2), as an alternative ammonia detoxification pathway[24, 25].

There were no significant changes in the expression of NOS isoforms in the kidney (Fig. 5B), whereas inducible NOS (*Nos2*) was robustly increased in the liver of BDL mice, in line with findings by others[26]. These changes were paralleled by the increased enzyme activity of arginase, and a marked drop in the activity of endothelial NOS (Fig. 5. Panels C and D). Cyclic guanosine monophosphate (cGMP), a marker of NOS activity, decreased in the kidneys of BDL mice (Fig. 5E), suggesting impaired NO production that is likely a result of the depleted arginine pool. 3-Nitrotyrosine (3-NT) formation, a marker of peroxynitrite generation or more broadly nitrative stress[27], was also increased around the dilated tubules in BDL mice (Fig. 5F), consistent with decreased NO availability and enhanced protein oxidation/nitration.

Genetic deletion of arginase-2 attenuates the development of renal injury in BDL mice

We further investigated the role of disturbed arginine metabolism in renal injury by using *Arg2*$^{-/-}$) and corresponding wild type (WT) mice. Despite the similar levels of liver injury (Fig. 6A), inflammatory cytokines, fibrotic markers (data not shown) and serum ALT (Fig. 6B) in the two strains, blood urea nitrogen and creatinine were significantly lower in the *Arg2*−/− mice (Fig. 6B), suggesting better preservation of renal function. Consistently, tubular architecture was also better preserved with less tubulointerstitial fibrosis in *Arg2*$^{-/-}$ compared to WT mice (Fig. 6C). Furthermore, BDL resulted in a smaller reduction in cortical microcirculation in *Arg2*$^{-/-}$ than in WT mice (Fig. 6DE). At the same time, the significant drop in liver microcirculation induced by BDL was similar in *Arg2*$^{-/-}$ and WT mice (Suppl. Fig. 3AB).

Hyperammonemia triggers the upregulation of arginase-2 and markers of tubular injury in human proximal tubular epithelial cells

In further *in vitro* experiments we tested whether ammonia *per se* canalter the expression of arginases and tubular-injury markers. Human renal proximal tubular epithelial cells (RPTEC) treated with ammonia showed a concentration-dependent upregulation of arginase-2, while arginase-1 was not detectable in these cells (Fig. 7A). Arginase-2 expression remained unchanged in the presence of 100 ng/mL endotoxin, suggesting inflammation-independent induction of arginase-2 by hyperammonemia. Furthermore, a high concentration of ammonia significantly reduced the expression of proximal tubular-specific claudin-2 (*Cldn2*)(28) and megalin (*Lrp2*), and increased lipocalin 2 (*Lcn2*) expression (Fig. 7C). However, the expression of arginase-2 was unaffected by any of the treatments in human umbilical vein endothelial cells (HUVEC) (Fig. 7B).

We also tested the effects of the 3 most common bile acids detectable in the serum of BDL animals at pmol/mL amounts(12) on arginase-2 expression in RPTEC. Only chenodeoxycholic acid at the highest 100 uM concentration, but not cholic acid and taurocholic acid at 1 and 100 uM concentrations, increased the expression of *Arg2* (Suppl. Fig. 4).

Discussion

Here we propose a novel mechanism by which kidney injury develops in HRS, based on findings in BDL mice. In this model, pathological changes in the kidney closely resemble the histopathological findings in the kidneys of patients with HRS. Our key finding is that the disruption of renal arginine metabolism plays a significant role in the development of renal pathology in HRS. We show that 1) BDL leads to progressive renal tubular injury that is likely related to impaired microvascular function as a consequence of decreased NO availability; 2) BDL-induced liver failure results in hyperammonemia, and a shift in the expression of ammonia detoxifying enzymes both in the liver and kidney, leading to decreased *de novo* production as well as increased breakdown of arginine in the kidneys; 3) genetic deletion of arginase-2 mitigates the development of kidney injury, and protects renal microcirculation in BDL mice; 4) arginase-2 is selectively upregulated in human proximal tubular cells by hyperammonemia.

Rapid deterioration of renal function due to AKI in end-stage liver disease is a life-threatening complication, which often develops on the background of HRS[29]. Concomitant infections, extreme jaundice and intrahepatic cholestasis contribute to the acute decompensation of cirrhosis and consequently to the development of kidney injury[3]. In BDL mice, all these factors that contribute to decompensation are present and rapidly progressing[30], which makes this a suitable model of kidney injury associated with cholestatic liver failure[12]. Hyperammonemia is another common feature of parenchymal liver failure, and is closely linked to impaired central neural function, known as hepatic encephalopathy. Hyperammonemia has also been recently recognized as a contributing factor in the development of complications of advanced liver cirrhosis. Hyperammonemia leads to activation of myostatin via NF-κB and thereby promoting sarcopenia[31], while the normalization of ammonia levels helps to restore skeletal muscle mass and function[32]. In elegant studies, Jalan *et al.* described how hyperammonemia leads to activation of hepatic stellate cells *in vitro* and promotes cirrhosis *in vivo* by triggering free radical production and endoplasmic reticulum stress in hepatic stellate cells[33]. The same group showed that ammonia *per se* is capable to negatively influencing neutrophil phagocytic function, thus increasing the susceptibility to infections in liver failure[34]. However, a potential direct effect of hyperammonemia on tubular epithelium has not yet been explored. We hypothesized that hyperammonemia might also contribute to renal pathology seen in bile duct-ligated mice. The central role of the kidneys in *de novo* arginine synthesis and the close link of this biosynthetic pathway with ammonia detoxifying enzymes(Fig. 4A) led us to investigate the renal expression of urea cycle enzymes, and to measure serum levels of amino acids as markers of systemic arginine homeostasis. Or results clearly indicate that BDL mice are in a systemic arginine-deficient state as a result of disturbed renal arginine production and increased arginine breakdown by arginase-2.

The human body is not able to produce sufficient amounts of arginine, especially when there is increased arginine need, making it a semi-essential amino acid, which is also an important substrate for NO synthases. Sepsis and other pro-inflammatory conditions are associated with arginine deficiency[35], which results in impaired function of eNOS[27], a likely contributor to poor outcomes in septic patients[27, 36]. During pro-inflammatory conditions, NO synthases and arginases are both induced by specific cytokines. Arginase activity (mainly as a result of arginase-1 upregulation) is triggered by Th2 cytokines, such as IL-4, IL-10 and IL-13, while NO synthase expression is triggered by TLR4 activation and by Th1 and Th17 cytokines. In theory, decreased arginine availability in pro-inflammatory states might function as a protective mechanism to counteract inducible NO synthase activity and to decrease excessive and damaging NO production. However, this might impair inflammation resolving processes by T-cells and macrophages[37–39], and may also impair microvascular functions by decreasing eNOS activity/function[40]. Indeed, in the present experiments arginine pool depletion was associated with impaired renal microcirculation accompanied by a pro-inflammatory state both in the liver and kidneys. The impaired renal microcirculation in BDL was also accompanied my markedly decreased eNOS activity in the kidneys. Notably, under pro-inflammatory conditions NO synthases may also be uncoupled and produce superoxide rather than NO, which fuels oxidative and nitrative stress promoting endothelial and parenchymal injury[27].

We identified arginase-2 in the kidneys as a major cause of arginine depletion. Global genetic deletion of arginase-2 was associated with better preserved renal architecture, better kidney functions, and maintained renal microvascular flow. These results are in line with published data showing preserved renal function and better microvascular flow in diabetic arginase-2 knockout mice, as well as in diabetic mice treated with the non-selective arginase inhibitor S-(2-boronoethyl)-L-cysteine[41]. The beneficial effect of arginase inhibition on microvascular flow in diabetics has also been recently documented in small clinical studies[42]. It would be intriguing to test whether pharmacological arginase-2 inhibition could attenuate kidney injury in HRS. Although several potent arginase inhibitors have recently been developed, none of them are specific for individual isoforms[40]. This limits their potential value in the treatment of liver failure, considering the crucial role of arginase-1 in hepatic ammonia detoxification[43].

We also show that ammonia can upregulate arginase-2 in human proximal tubular epithelial cells, with concomitant induction of tubular injury markers and a reduction in markers of tubular function. Thus, ammonia in concert with multiple other potential factors (inflammation, oxidative/nitrative stress, bile acids) may contribute to arginine deficiency and decreased eNOS activity, promoting microcirculatory dysfunction/injury, tissue hypoxia, and tubular damage accompanied by inflammation.

Collectively, our results highlight the importance of interorgan alterations in arginine metabolism in the development of renal injury in HRS and suggest that bile duct-ligation in mice is a translational model of HRS.

Supplementary Material

Refer to Web version on PubMed Central for supplementary material.

Acknowledgments

This work was supported by the Intramural Research Program of NIAAA/NIH (to P. Pacher, and G. Kunos). C. Matyas was supported by a scholarship of the Hungarian-American Enterprise Scholarship Fund/Council on International Educational Exchange. Z. V. Varga was supported by the Rosztoczy Foundation.

Abbreviations used

AKI	acute kidney injury
ALT	alanine aminotransferase
ALKP	alkaline phosphatase
Angpt1	angiopoietin 1
ARG1	arginase-1
ARG2	arginase-2
ASL	argininosuccinate lyase
ASS1	argininosuccinate synthase 1
BDL	bile duct-ligation
BUN	blood urea nitrogen
Cdh5	VE-cadherin
cGMP	Ccl2, monocyte chemoattractant protein 1/MCP-1
Ccl3	macrophage inflammatory protein 1-alpha/MIP-1-α
Cxcl2	macrophage inflammatory protein 2-alpha/MIP2; cyclic guanosine monophosphate
Cldn22	claudin
Col1a1	collagen 1
Col3a1	collagen 3
Cps1	carbamoyl-phosphate synthetase 1
Cubn	Cubilin
DAB	diaminobenzidine
eNOS/NOS3	endothelial nitric oxide synthase
Fabp1	fatty acid binding protein 1

Flt1	vascular endothelial growth factor receptor 1
Gls1	glutaminase 1
Gls2	glutaminase 2
Glud1	glutamate dehydrogenase
Glul	glutamine synthetase
H2O2	hydrogen peroxide
H&E	hematoxylin and eosin
Hif1a	hypoxia-inducible factor 1-alpha
HRS	hepatorenal syndrome
Icam1	intercellular adhesion molecule 1
Il1b	Interleukin 1 beta/IL-1β
Il6	Interleukin 6/IL-6
Kdr	vascular endothelial growth factor receptor 2
KIM-1	kidney injury molecule 1/Havcr1
Lcn2	lipocalin2
LPS	lipopolysaccharide
Lrp2	megalin
mRNA	messenger RNA
NF-κB	nuclear factor kappa-light-chain-enhancer of activated B cells
NOS	nitric oxide synthase
Otc	ornithine transcarbamylase
PAS	periodic acid-Schiff stain
PBS	phosphate buffered saline
PCR	polymerase chain reaction
Pecam1	platelet endothelial cell adhesion molecule 1
RPTEC	human renal proximal tubular epithelial cells
Sele	E-selectin
Selp	P-selectin
Slc34a2	sodium-dependent phosphate transport protein 2A

Slc5a2	sodium/glucose cotransporter 2/SGLT2
TGF-β	transforming growth factor-beta1
Tie1	tyrosine kinase with immunoglobulin-like and EGF-like domains 1
Tnf	tumor necrosis factor/TNF-α
Vcam1	vascular cell adhesion molecule 1
Vegfa	vascular endothelial growth factor A
Vim	vimentin
WT	wild type

References

1. Blachier M, Leleu H, Peck-Radosavljevic M, Valla DC, Roudot-Thoraval F. The burden of liver disease in Europe: a review of available epidemiological data. J Hepatol. 2013; 58:593–608. [PubMed: 23419824]
2. Pericleous M, Sarnowski A, Moore A, Fijten R, Zaman M. The clinical management of abdominal ascites, spontaneous bacterial peritonitis and hepatorenal syndrome: a review of current guidelines and recommendations. Eur J Gastroenterol Hepatol. 2016; 28:e10–18. [PubMed: 26671516]
3. Davenport A, Sheikh MF, Lamb E, Agarwal B, Jalan R. Acute kidney injury in acute-on-chronic liver failure: where does hepatorenal syndrome fit? Kidney Int. 2017; 92(5):1058–1070. [PubMed: 28844314]
4. Garcia-Tsao G, Parikh CR, Viola A. Acute kidney injury in cirrhosis. Hepatology. 2008; 48:2064–2077. [PubMed: 19003880]
5. Cardenas A, Gines P, Uriz J, Bessa X, Salmeron JM, Mas A, Ortega R, et al. Renal failure after upper gastrointestinal bleeding in cirrhosis: incidence, clinical course, predictive factors, and short-term prognosis. Hepatology. 2001; 34:671–676. [PubMed: 11584362]
6. Fabrizi F, Messa P. Challenges in Renal Failure Treatment Before Liver Transplant. Clin Liver Dis. 2017; 21:303–319. [PubMed: 28364815]
7. Bernardi M, Moreau R, Angeli P, Schnabl B, Arroyo V. Mechanisms of decompensation and organ failure in cirrhosis: From peripheral arterial vasodilation to systemic inflammation hypothesis. J Hepatol. 2015; 63:1272–1284. [PubMed: 26192220]
8. Arroyo V. Microalbuminuria, systemic inflammation, and multiorgan dysfunction in decompensated cirrhosis: evidence for a nonfunctional mechanism of hepatorenal syndrome. Hepatol Int. 2017; 11:242–244. [PubMed: 28124314]
9. Mocarzel LO, Bicca J, Jarske L, Oliveira T, Lanzieri P, Gismondi R, Ribeiro ML. Cirrhotic Cardiomyopathy: Another Case of a Successful Approach to Treatment of Hepatorenal Syndrome. Case Rep Gastroenterol. 2016; 10:531–537. [PubMed: 27843430]
10. Acevedo J, Fernandez J, Prado V, Silva A, Castro M, Pavesi M, Roca D, et al. Relative adrenal insufficiency in decompensated cirrhosis: Relationship to short-term risk of severe sepsis, hepatorenal syndrome, and death. Hepatology. 2013; 58:1757–1765. [PubMed: 23728792]
11. Fickert P, Krones E, Pollheimer MJ, Thueringer A, Moustafa T, Silbert D, Halilbasic E, et al. Bile acids trigger cholemic nephropathy in common bile-duct-ligated mice. Hepatology. 2013; 58:2056–2069. [PubMed: 23813550]
12. Krones E, Eller K, Pollheimer MJ, Racedo S, Kirsch AH, Frauscher B, Wahlstrom A, et al. NorUrsodeoxycholic acid ameliorates cholemic nephropathy in bile duct ligated mice. J Hepatol. 2017; 67:110–119. [PubMed: 28242240]
13. van Slambrouck CM, Salem F, Meehan SM, Chang A. Bile cast nephropathy is a common pathologic finding for kidney injury associated with severe liver dysfunction. Kidney Int. 2013; 84:192–197. [PubMed: 23486516]

14. Okamura Y, Hata K, Inamoto O, Kubota T, Hirao H, Tanaka H, Fujimoto Y, et al. Influence of hepatorenal syndrome on outcome of living donor liver transplantation: A single-center experience in 357 patients. Hepatol Res. 2017; 47:425–434. [PubMed: 27323334]
15. Mukhopadhyay P, Rajesh M, Cao Z, Horvath B, Park O, Wang H, Erdelyi K, et al. Poly (ADP-ribose) polymerase-1 is a key mediator of liver inflammation and fibrosis. Hepatology. 2014; 59:1998–2009. [PubMed: 24089324]
16. Fine LG, Bandyopadhay D, Norman JT. Is there a common mechanism for the progression of different types of renal diseases other than proteinuria? Towards the unifying theme of chronic hypoxia Kidney. Int Suppl. 2000; 75:S22–26.
17. Orphanides C, Fine LG, Norman JT. Hypoxia stimulates proximal tubular cell matrix production via a TGF-beta1-independent mechanism. Kidney Int. 1997; 52:637–647. [PubMed: 9291182]
18. Norman JT, Clark IM, Garcia PL. Hypoxia promotes fibrogenesis in human renal fibroblasts. Kidney Int. 2000; 58:2351–2366. [PubMed: 11115069]
19. Bullen JW, Tchernyshyov I, Holewinski RJ, DeVine L, Wu F, Venkatraman V, Kass DL, et al. Protein kinase A-dependent phosphorylation stimulates the transcriptional activity of hypoxia-inducible factor 1. Sci Signal. 2016; 9:ra56. [PubMed: 27245613]
20. Suzuki H, Tomida A, Tsuruo T. Dephosphorylated hypoxia-inducible factor 1alpha as a mediator of p53-dependent apoptosis during hypoxia. Oncogene. 2001; 20:5779–5788. [PubMed: 11593383]
21. van de Poll MC, Siroen MP, van Leeuwen PA, Soeters PB, Melis GC, Boelens PG, Deutz NE, et al. Interorgan amino acid exchange in humans: consequences for arginine and citrulline metabolism. Am J Clin Nutr. 2007; 85:167–172. [PubMed: 17209193]
22. Adeva MM, Souto G, Blanco N, Donapetry C. Ammonium metabolism in humans. Metabolism. 2012; 61:1495–1511. [PubMed: 22921946]
23. Wright G, Noiret L, Olde Damink SW, Jalan R. Interorgan ammonia metabolism in liver failure: the basis of current and future therapies. Liver Int. 2011; 31:163–175. [PubMed: 20673233]
24. Dasarathy S, Merli M. Sarcopenia from mechanism to diagnosis and treatment in liver disease. J Hepatol. 2016; 65:1232–1244. [PubMed: 27515775]
25. Davuluri G, Krokowski D, Guan BJ, Kumar A, Thapaliya S, Singh D, Hatzoglou M, et al. Metabolic adaptation of skeletal muscle to hyperammonemia drives the beneficial effects of l-leucine in cirrhosis. J Hepatol. 2016; 65:929–937. [PubMed: 27318325]
26. Cinar R, Iyer MR, Liu Z, Cao Z, Jourdan T, Erdelyi K, Godlewski G, et al. Hybrid inhibitor of peripheral cannabinoid-1 receptors and inducible nitric oxide synthase mitigates liver fibrosis. JCI Insight. 2016; 1(11) pii: e87336.
27. Pacher P, Beckman JS, Liaudet L. Nitric oxide and peroxynitrite in health and disease. Physiol Rev. 2007; 87:315–424. [PubMed: 17237348]
28. Enck AH, Berger UV, Yu AS. Claudin-2 is selectively expressed in proximal nephron in mouse kidney. Am J Physiol Renal Physiol. 2001; 281:F966–974. [PubMed: 11592954]
29. Belcher JM, Garcia-Tsao G, Sanyal AJ, Bhogal H, Lim JK, Ansari N, Coca SG, et al. Association of AKI with mortality and complications in hospitalized patients with cirrhosis. Hepatology. 2013; 57:753–762. [PubMed: 22454364]
30. O'Brien A, China L, Massey KA, Nicolaou A, Winstanley A, Newson J, Hobbs A, et al. Bile duct-ligated mice exhibit multiple phenotypic similarities to acute decompensation patients despite histological differences. Liver Int. 2016; 36:837–846. [PubMed: 26012885]
31. Qiu J, Thapaliya S, Runkana A, Yang Y, Tsien C, Mohan ML, Narayanan A, et al. Hyperammonemia in cirrhosis induces transcriptional regulation of myostatin by an NF-kappaB-mediated mechanism. Proc Natl Acad Sci U S A. 2013; 110:18162–18167. [PubMed: 24145431]
32. Kumar A, Davuluri G, Silva RNE, Engelen M, Ten Have GAM, Prayson R, Deutz NEP, et al. Ammonia lowering reverses sarcopenia of cirrhosis by restoring skeletal muscle proteostasis. Hepatology. 2017; 65:2045–2058. [PubMed: 28195332]
33. Jalan R, De Chiara F, Balasubramaniyan V, Andreola F, Khetan V, Malago M, Pinzani M, et al. Ammonia produces pathological changes in human hepatic stellate cells and is a target for therapy of portal hypertension. J Hepatol. 2016; 64:823–833. [PubMed: 26654994]

34. Shawcross DL, Wright GA, Stadlbauer V, Hodges SJ, Davies NA, Wheeler-Jones C, Pitsillides AA, et al. Ammonia impairs neutrophil phagocytic function in liver disease. Hepatology. 2008; 48:1202–1212. [PubMed: 18697192]

35. Davis JS, Anstey NM. Is plasma arginine concentration decreased in patients with sepsis? A systematic review and meta-analysis. Crit Care Med. 2011; 39:380–385. [PubMed: 21150584]

36. Luiking YC, Poeze M, Dejong CH, Ramsay G, Deutz NE. Sepsis: an arginine deficiency state? Crit Care Med. 2004; 32:2135–2145. [PubMed: 15483426]

37. Bronte V, Zanovello P. Regulation of immune responses by L-arginine metabolism. Nat Rev Immunol. 2005; 5:641–654. [PubMed: 16056256]

38. Feldmeyer N, Wabnitz G, Leicht S, Luckner-Minden C, Schiller M, Franz T, Conradi R, et al. Arginine deficiency leads to impaired cofilin dephosphorylation in activated human T lymphocytes. Int Immunol. 2012; 24:303–313. [PubMed: 22345165]

39. Bronte V, Serafini P, Mazzoni A, Segal DM, Zanovello P. L-arginine metabolism in myeloid cells controls T-lymphocyte functions. Trends Immunol. 2003; 24:302–306. [PubMed: 12810105]

40. Caldwell RB, Toque HA, Narayanan SP, Caldwell RW. Arginase: an old enzyme with new tricks. Trends Pharmacol Sci. 2015; 36:395–405. [PubMed: 25930708]

41. Morris SM Jr, Gao T, Cooper TK, Kepka-Lenhart D, Awad AS. Arginase-2 mediates diabetic renal injury. Diabetes. 2011; 60:3015–3022. [PubMed: 21926276]

42. Kovamees O, Shemyakin A, Checa A, Wheelock CE, Lundberg JO, Ostenson CG, Pernow J. Arginase Inhibition Improves Microvascular Endothelial Function in Patients With Type 2 Diabetes Mellitus. J Clin Endocrinol Metab. 2016; 101:3952–3958. [PubMed: 27399350]

43. Ballantyne LL, Sin YY, Al-Dirbashi OY, Li X, Hurlbut DJ, Funk CD. Liver-specific knockout of arginase-1 leads to a profound phenotype similar to inducible whole body arginase-1 deficiency. Mol Genet Metab Rep. 2016; 9:54–60. [PubMed: 27761413]

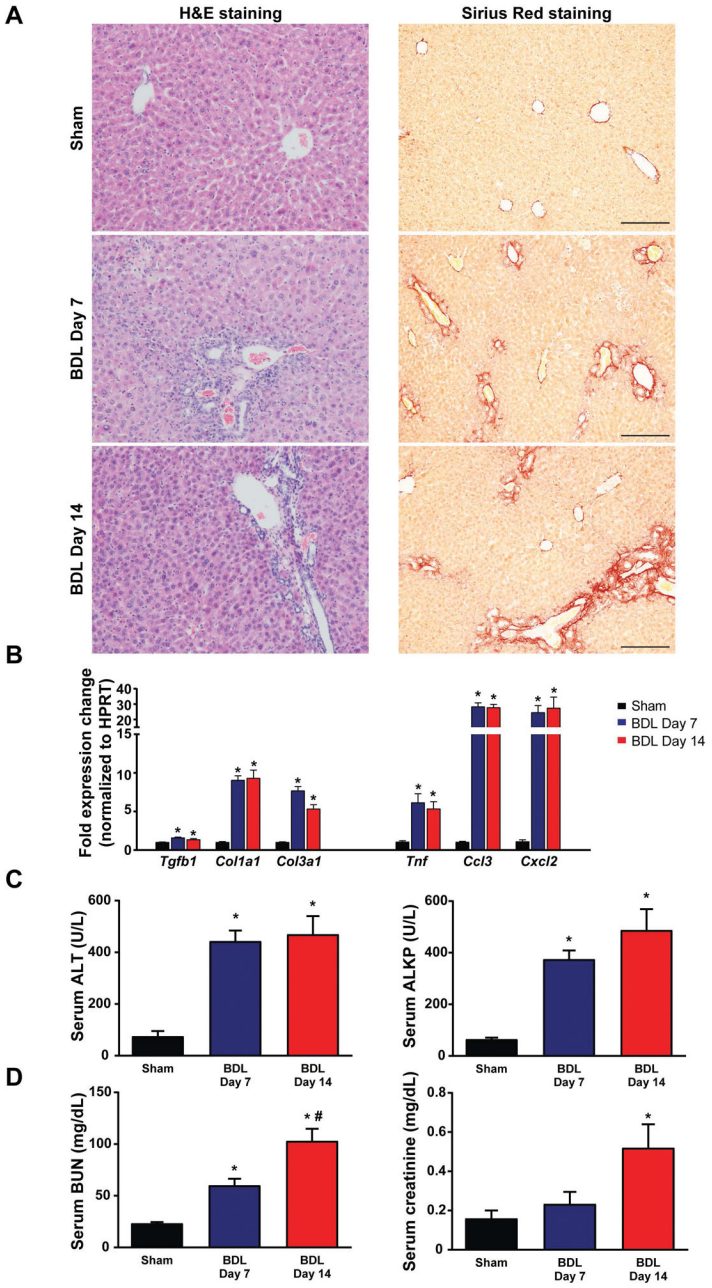

Fig. 1. Time-dependent changes in the markers of liver inflammation and fibrosis in bile duct-ligated mice

(**A**) Histological assessment of hepatic necrosis, and fibrosis in BDL mice. Scale bar represent 200 μm. (**B**) Expression of fibrotic markers TGF-β(*Tgfb1*), collagen 1(*Col1a1*), collagen 3(*Col3a1*) and inflammatory markers TNF-α(*Tnf*), MIP-1-α(*Ccl3*), MIP2(*Cxcl2*), in livers of sham operated mice (Sham) or in mice subjected to BDL and sacrificed on postoperative day 7 (BDL Day 7) or day 14 (BDL Day 14), respectively. (**C**) Enzymatic markers of liver and (**D**) kidney injury. Results are mean±S.E.M. *p<0.05 vs. sham #p<0.05 vs. BDL Day 7, n=5–6.

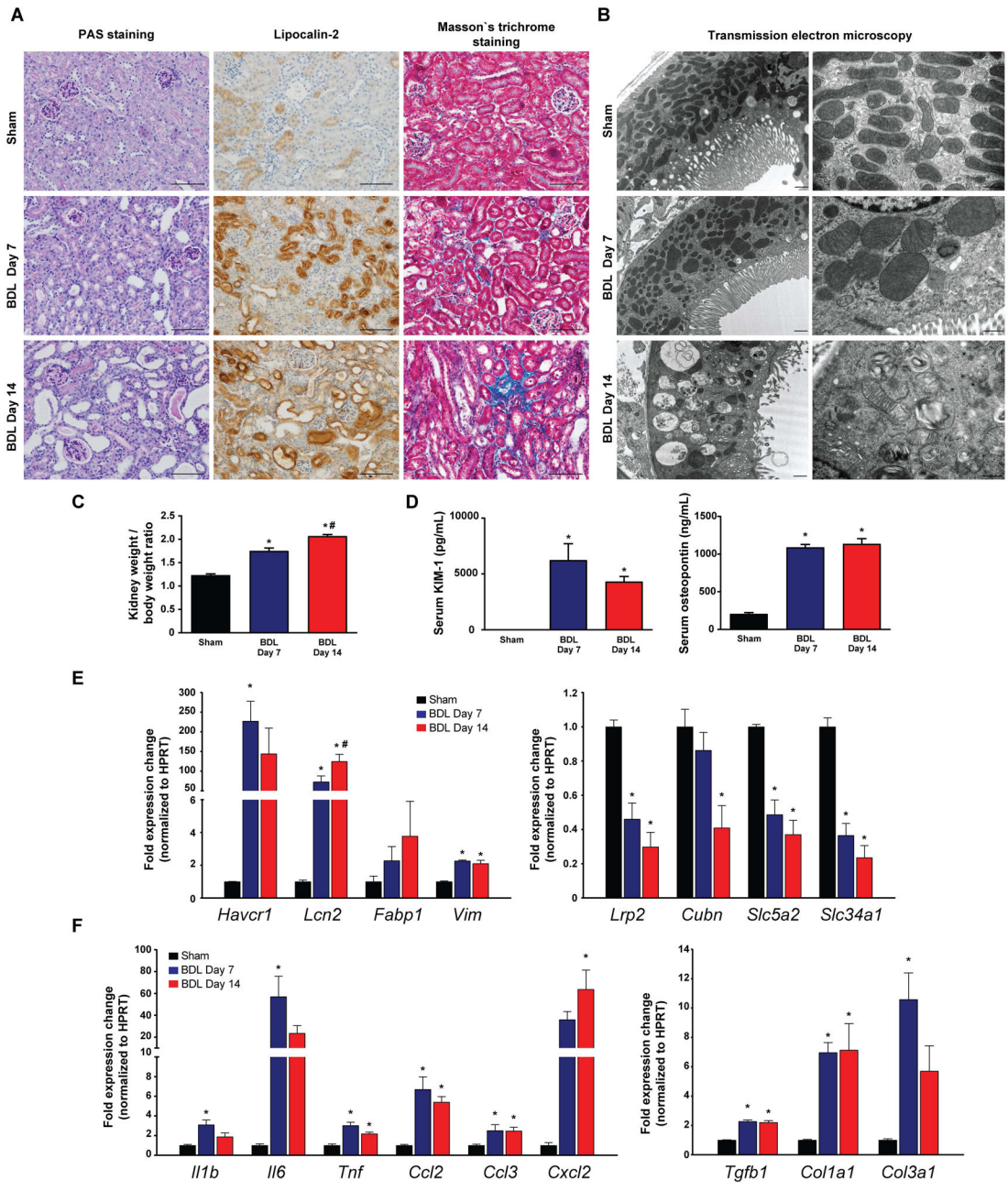

Fig. 2. Bile duct-ligation induces massive tubular damage

(**A**) Histological assessment of tubular injury (PAS staining, and lipocalin-2 immunohistochemistry), as well as tubulointerstitial fibrosis (Masson's trichrome staining). Scale bar represent 100 μm. (**B**) Transmission electron microscopic images of proximal tubular epithelial cells. Original magnification on left panels are 10,000X; high power fields are 25,000X. (**C**) Kidney/body weight ratio during the course of study. (**D**) Serum KIM-1 and osteopontin protein levels of sham operated mice (Sham) or of mice subjected to BDL and sacrificed on postoperative day 7 (BDL Day 7) or day 14 (BDL Day 14), respectively. (**E**) Expression of tubular injury markers KIM-1 (*Havcr1*), Lipocalin-2 (*Lcn2*), fatty acid

binding protein 1 (*Fabp1*) and vimentin (*Vim*), and genes involved in absorptive function of proximal tubuli megalin (*Lrp2*), cubilin (*Cubn*), SGLT2 (*Slc5a2*), and sodium-dependent phosphate transport protein 2A (*Slc34a2*) in kidneys of sham operated mice (Sham) or mice subjected to BDL and sacrificed on postoperative day 7 (BDL Day 7) or day 14 (BDL Day 14), respectively. (**F**) Expression of inflammatory markers IL-1β(*Il1b*), IL-6(*Il6*), TNF-α(*Tnf*), MCP-1(*Ccl2*), MIP-1-α(*Ccl3*), MIP2(*Cxcl2*), and expression of fibrotic markers TGF-β(*Tgfb1*), collagen 1(*Col1a1*), collagen 3(*Col3a1*), in kidneys of sham operated mice (Sham) or in mice subjected to BDL and sacrificed on postoperative day 7 (BDL Day 7) or day 14 (BDL Day 14), respectively. Results are mean±S.E.M. *$p<0.05$ vs. sham, n=6.

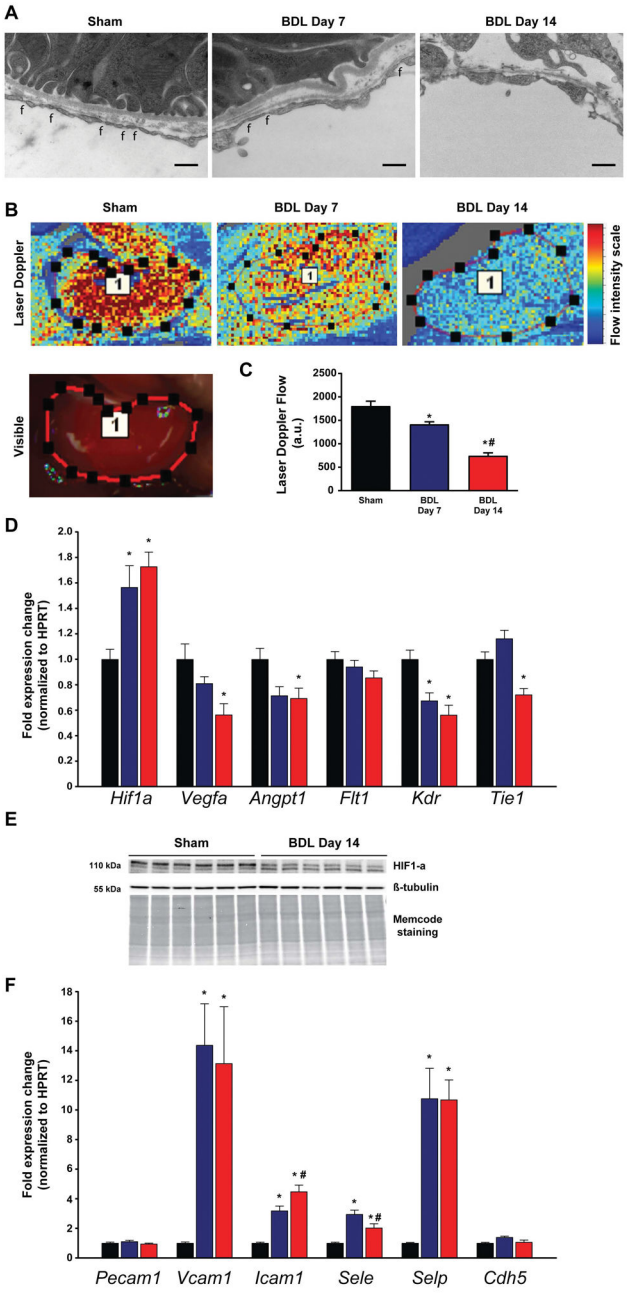

Fig. 3. Impaired renal microcirculation, and vascular inflammation leads to tubular hypoxia

(**A**) Transmission electron microscopic images of peritubular endothelial cells. Original magnification is 25,000X, scale bar represents 400 nm, f: fenestrations. (**B**) Representative illustration of renal microcirculation by Laser speckle contrast analysis. (**C**) Quantification of renal microvascular flow. (**D**) Gene expression of hypoxia-inducible factor 1-alpha(*Hif1a*), vascular endothelial growth factor A(*Vegfa*), angiopoietin 1(*Angpt1*), vascular endothelial growth factor receptor 1(*Flt1*), vascular endothelial growth factor receptor 2(*Kdr*), and tyrosine kinase with immunoglobulin-like and EGF-like domains 1(*Tie1*). (**E**) Hypoxia-inducible factor 1-alpha(HIF1α) protein expression analysis by Western blot. (**F**)

Expression of vascular adhesion molecules platelet endothelial cell adhesion molecule 1(*Pecam1*), vascular cell adhesion molecule 1(*Vcam1*), intercellular adhesion molecule 1(*Icam1*), E-selectin(*Sele*), P-selectin(*Selp*), and VE-cadherin(*Cdh5*) in sham operated mice (Sham) or in mice subjected toBDL and sacrificed on postoperative day 7 (BDL Day 7) or day 14 (BDL Day 14), respectively. Results are mean±S.E.M. *$p<0.05$ vs. sham #$p<0.05$ vs. BDL Day 7, n=6.

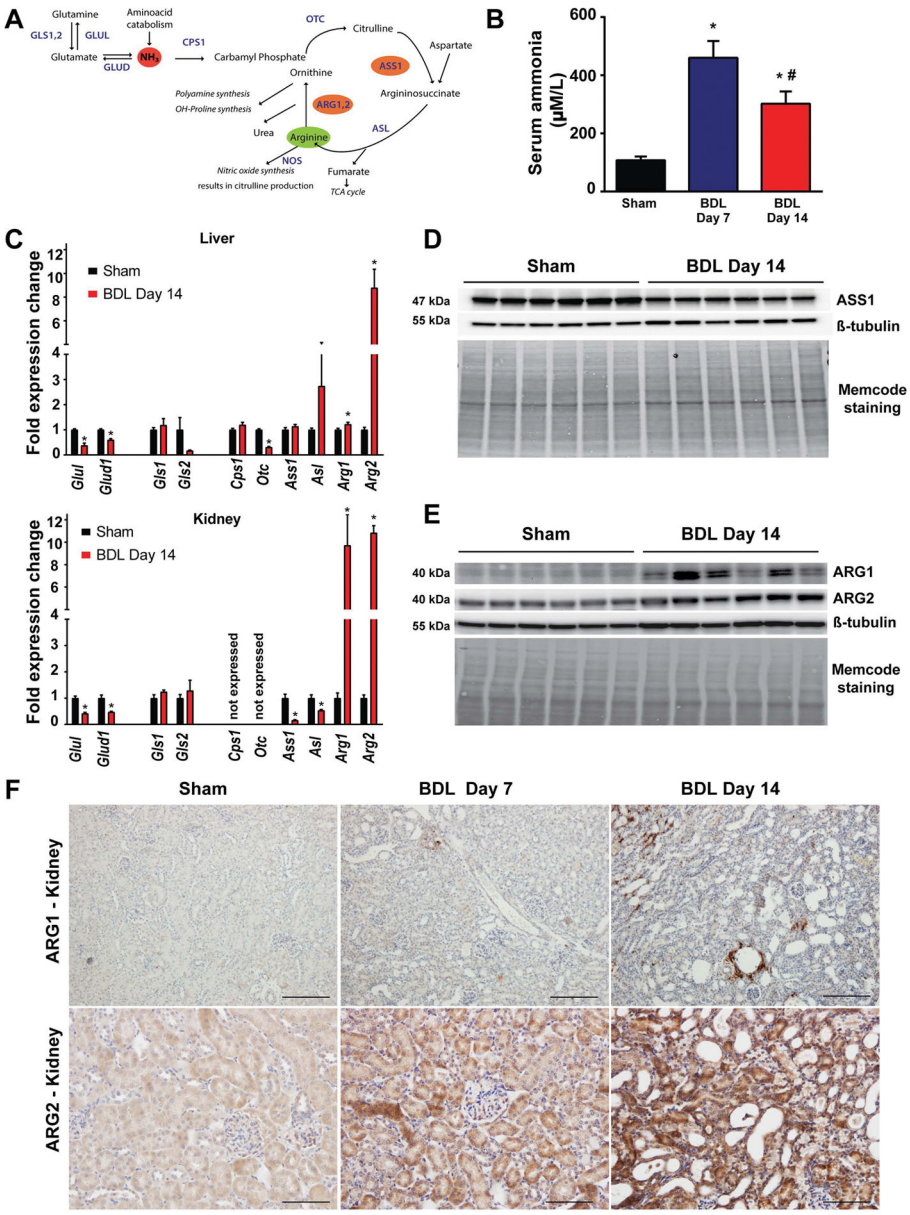

Fig. 4. Disruption of renal arginine metabolism in bile duct-ligated mice

(**A**) Schematic representation of pathways involved in arginine metabolism. (**B**) Serum ammonia levels and (**C**) hepatic and renal expression of genes involved in ammonia detoxification: glutamine synthetase(*Glul*), glutamate dehydrogenase(*Glud1*), glutaminase 1(*Gls1*), glutaminase 2(*Gls2*), carbamoyl-phosphate synthetase 1(*Cps1*), ornithine transcarbamylase(*Otc*), argininosuccinate synthase 1(*Ass1*), argininosuccinate lyase(*Asl*), arginase 1(*Arg1*), and arginase 2(*Arg2*) of sham operated mice (Sham) or of mice subjected to BDL and sacrificed on postoperative day 14 (BDL Day 14). (**D**) Argininosuccinate synthase (ASS1) protein expression analysis by Western blot and (**E**) Arginase-1 (ARG1) and Arginase-2 (ARG2) protein expression analysis by Western blot in sham operated mice (Sham) or in mice subjected to BDL and sacrificed on postoperative day 14 (BDL Day 14).

β-tubulin and total protein staining (Memcode staining) is shown as loading controls. (**F**) Arginase-1 and Arginase-2 protein expression analysis by immunostaining in sham operated mice (Sham) or in mice subjected to BDL and sacrificed on postoperative day 7 (BDL Day 7) or day 14 (BDL Day 14), respectively. Scale bar represent 100 μm. Results are mean ±S.E.M. *$p<0.05$ vs. sham, n=6.

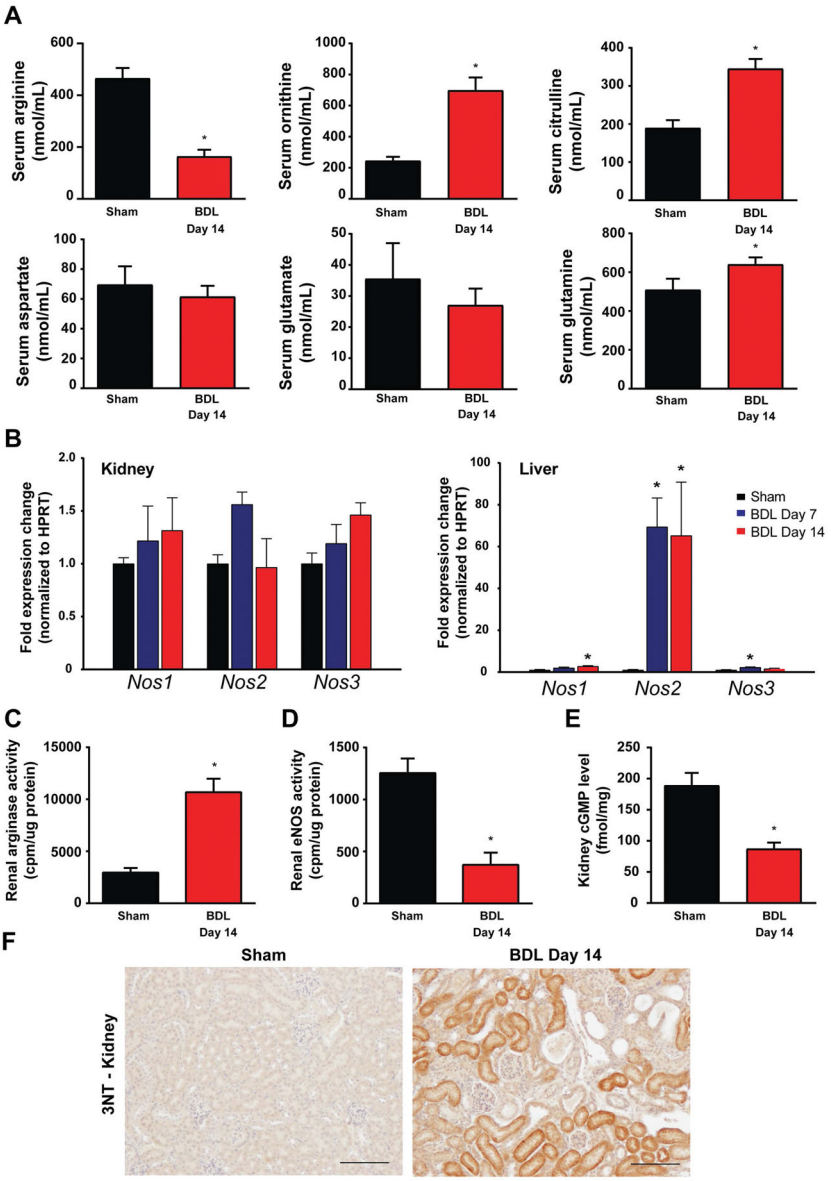

Fig. 5. Serum levels of arginine metabolism-related amino acids in bile duct-ligated mice

(**A**) Serum levels of arginine, ornithine, citrulline, aspartate, glutamate, and glutamine in sham operated mice (Sham) or in mice subjected to BDL and sacrificed on postoperative day 14 (BDL Day 14). (**B**) Renal and hepatic expression of nitric oxide synthase isoforms: Nos1–neuronal, Nos2–inducible, Nos3–endothelial, in sham operated mice (Sham–black bars) or in mice subjected to bile duct-ligation and sacrificed on postoperative day 7 (BDL Day 7–blue bars) or day 14 (BDL Day 14–red bars), respectively. Enzyme activity of arginases (**C**), and endothelial nitric oxide synthase (**D**). (**E**) Renal levels of cyclic guanosine monophosphate (cGMP) in sham operated mice (Sham–black bars) or in mice subjected to bile duct-ligation and sacrificed on postoperative day 14 (BDL Day 14–red bars). (F) 3-nitrotyrosine (3-NT) expression analysis, as a marker of nitrative stress by immunostaining in sham operated mice (Sham) or in mice subjected to BDL and sacrificed on postoperative

day 14 (BDL Day 14). Scale bar represent 100 μm. Results are mean±S.E.M. *$p<0.05$ vs. sham, n=10–15 for amino acid analysis, n=6–8 in other experiments.

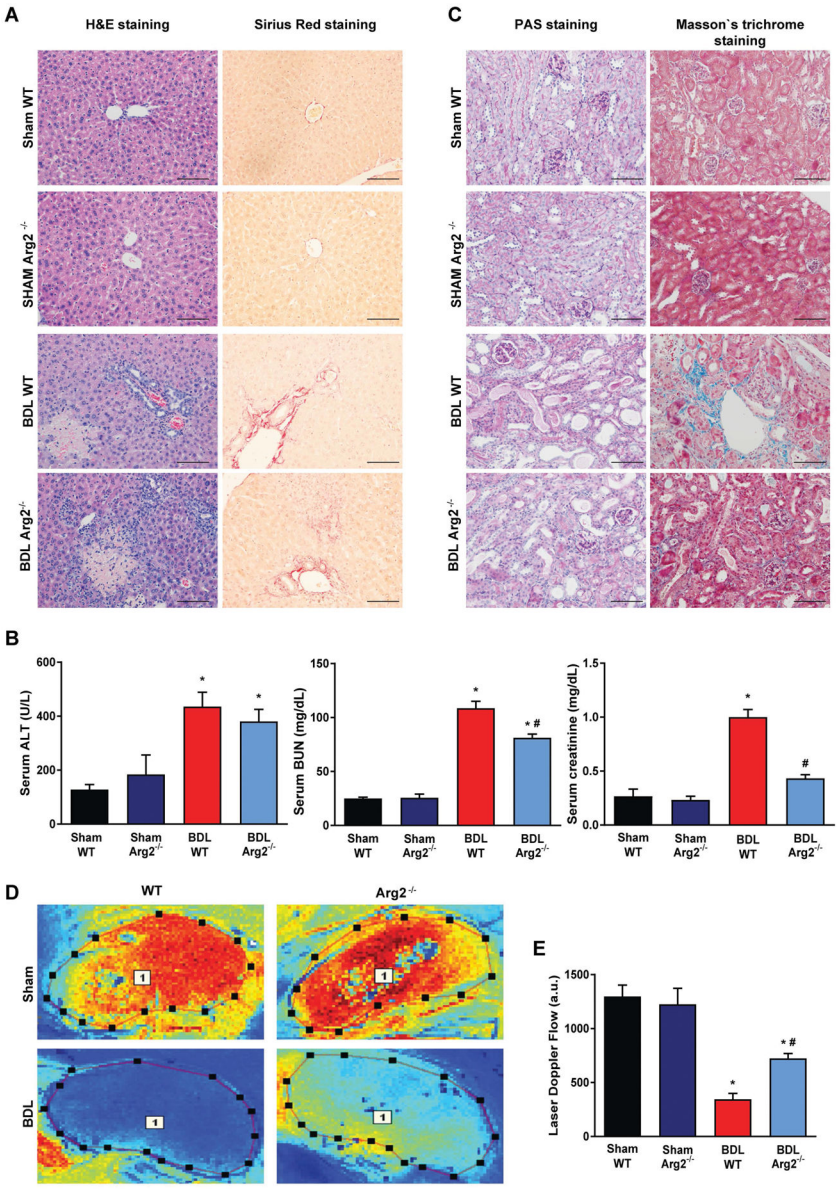

Fig. 6. Arginase-2 deficient mice are partially rescued from kidney injury in bile duct-ligated mice

(**A**) Histological assessment of hepatic necrosis, and fibrosis in sham operated wild type (Sham WT) or Arginase-2-deficient mice (Sham Arg2$^{-/-}$) or in wild type or Arginase-2-deficient mice subjected to bile duct-ligation and sacrificed on postoperative 14 (BDL WT, or BDL Arg2$^{-/-}$), respectively. Scale bar represent 100 μm. (**B**) Enzymatic markers of liver and kidney injury. (**C**) Histological assessment of tubular injury (PAS staining) and tubulointerstitial fibrosis (Masson's trichrome staining). Scale bar represent 100 μm. (**D**) Representative illustration of renal microcirculation assessment by Laser speckle contrast analysis. (**E**) Quantification of renal microvascular flow. Results are mean±S.E.M. *p<0.05 vs. Sham WT #p<0.05 vs. BDL WT, n=4–6.

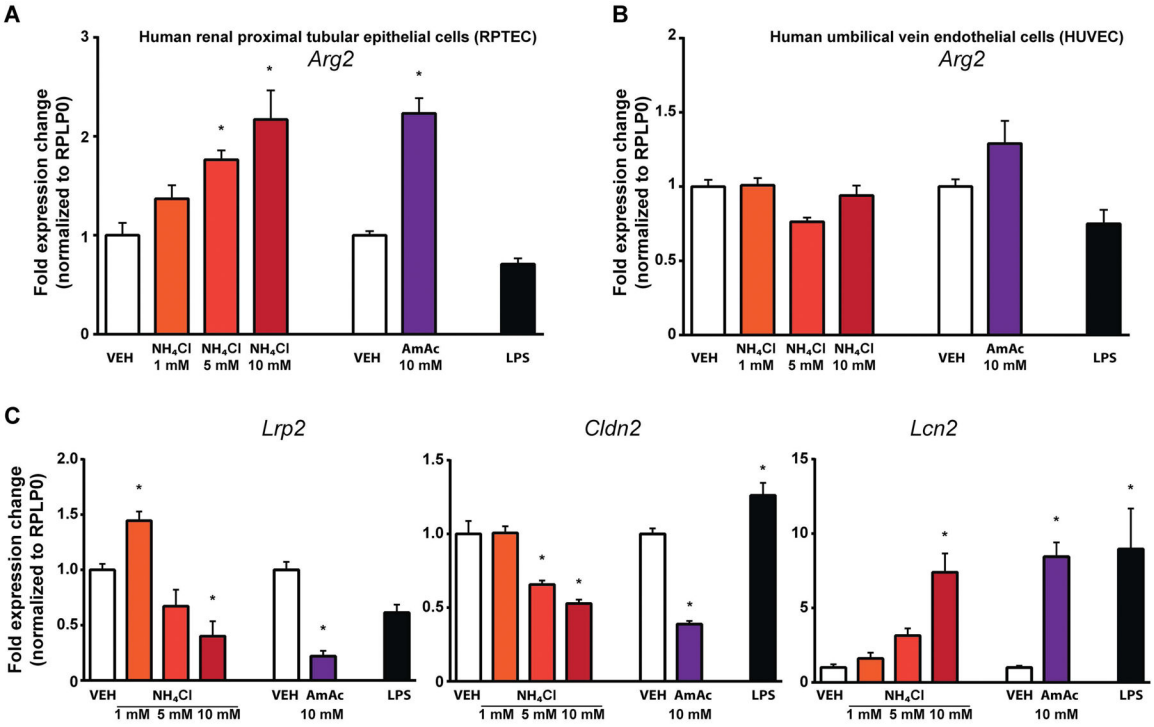

Fig. 7. Ammonia promotes tubular cell injury and the upregulation of arginase-2

(A) Arginase-2 (*Arg2*) expression in human proximal tubular cells exposed to either 1, 5, 10 mM NH_4Cl, or 10 mM ammonium acetate (AmAc) for 48 h or in the presence of E. Coli O55:B5 LPS (100 ng/mL–6h). (**B**) Arginase-2 (*Arg2*) expression in human umbilical vein endothelial cells exposed to either 1, 5, 10 mM NH_4Cl, or 10 mM ammonium acetate (AmAc) for 48 h or in the presence of E. Coli O55:B5 LPS (100 ng/mL–6h). (**C**) Megalin (*Lrp2*), Claudin (*Cldn2*), and Lipocalin-2 (*Lcn2*) gene expression in human proximal tubular cells exposed to either 1, 5, 10 mM NH_4Cl, or 10 mM ammonium acetate (AmAc) for 48 h or in the presence of E. Coli O55:B5 LPS (100 ng/mL–6h). Results are mean±S.E.M. *p<0.05 vs. vehicle control #p<0.05 vs. LPS treated vehicle control, n=7.